# Electron microprobe analysis of Ca in olivine close to grain boundaries: The problem of secondary X-ray fluorescence

## JOHN A. DALTON[1] AND STEPHEN J. LANE[2]

[1]Geosciences Program, University of Texas at Dallas, Box 830688, Richardson, Texas 75083-0688, U.S.A.
[2]Department of Geology, University of Bristol, Wills Memorial Building, Queens Road, Bristol BS8 1RJ, U.K.

## ABSTRACT

Analysis of Ca in olivine grains close to boundaries with Ca-rich phases is inherently problematic because of the effects of secondary X-ray fluorescence of Ca from the adjoining Ca-rich phase. Commercial fluorescence-correction methods assume chemical homogeneity throughout the entire interaction volume and yield enhanced Ca concentrations for the olivine in such cases. We have determined the effects of Fe content of the olivine and Ca content of the adjoining phase on the magnitude of secondary fluorescence effects during electron microprobe analysis of Ca in olivine.

Significant errors in Ca determination were observable at horizontal beam-interface distances ranging from 30 $\mu$m for an Fe-free olivine–diopside couple to 70 $\mu$m for an olivine ($Fo_{90.7}$)–calcite couple. In general, the beam-interface distance required to suppress secondary fluorescence of Ca X-rays from the adjoining phase increases with increasing Fe content of the olivine and Ca content of the neighboring phase. Analysis of an olivine ($Fo_{90.7}$) wedge mounted on a standard thin-section glass slide (5.06 wt% Ca) showed significant secondary fluorescence of Ca to a wedge depth approaching 20 $\mu$m. It is recommended that olivine grains be separated and remounted in a Ca-free matrix for the determination of Ca concentrations in olivine by electron microprobe analysis.

## INTRODUCTION

Electron microprobe analysis is based on the generation and detection of characteristic X-rays from a sample of unknown composition. X-rays are fluoresced primarily by ionization of the inner orbital electrons of sample atoms by high-energy electrons. Reed (1993) gives the diameter (in micrometers) for 99% generation of primary X-rays as

$$d = 0.231 \frac{(E_o^{1.5} - E_c^{1.5})}{\rho} \qquad (1)$$

where $E_o$ and $E_c$ are the electron beam and critical excitation energies (in kiloelectron volts), respectively, and $\rho$ is the sample density (in grams per cubic centimeter). Typical values of the 99% primary interaction volume diameter for 15 keV incident electrons in silicate minerals are 4–5 $\mu$m. This dimension is commonly taken as the spatial resolution in quantitative analysis.

Primary X-rays are emitted in all directions from the primary interaction volume. Those traveling within the sample are predominantly absorbed by the photoelectric effect resulting in the fluorescence of secondary X-rays. The range of primary X-rays within the sample is considerably larger than the range of incident electrons of comparable energy because the X-ray has no net electrostatic charge. This means that the interaction volume for secondary X-ray fluorescence is considerably larger than that for primary X-ray fluorescence (Green 1964). Secondary fluorescence is generated by both characteristic and continuum primary X-rays with energies greater than the critical excitation energy of the X-rays to be fluoresced. In the case of olivine, Ca characteristic $K$ X-rays are fluoresced by continuum X-rays with energy exceeding 4.037 keV and by Fe characteristic $K$ X-rays (6.398, 7.057 keV).

Secondary fluorescence produces only a minor and correctable enhancement of the detected X-ray signal provided the sample is chemically homogeneous throughout the secondary interaction volume. The effects of secondary fluorescence are most significant near a compositional boundary (Fig. 1) and are not correctable by conventional programs because the assumption of homogeneity in the matrix-correction procedure no longer applies. The errors are particularly prominent in the analysis of low concentrations of an element close to a boundary with a substance that contains significant quantities of the same element (Reed and Long 1963).

Geologically, such a situation is encountered in the analysis of Ca in olivine. First, olivine contains low concentrations (<1 wt%) of Ca (Simpkin and Smith 1970) but is frequently found adjoining very Ca-rich minerals such as clinopyroxene or plagioclase feldspar, and also Ca-bearing liquid in the case of experimental samples. Second, most olivine contains significant Fe concentrations, which could possibly cause characteristic fluorescence of Ca X-rays in the surrounding matrix by primary $FeK\alpha$ X-rays originating in the olivine. Therefore, care is

required in the analysis of olivine grains close to a boundary with a Ca-rich phase and also in the analysis of small grains. The latter situation is particularly relevant in experimental charges in which the grain size is often <30 μm.

Ca is a very important minor constituent of natural olivine. Early studies (Stormer 1973; Simpkin and Smith 1970) suggested that the commonly observed zonation profiles of Ca in olivine were in part controlled by the temperature history of the host magma. A knowledge of the diffusion coefficient of Ca in olivine (Jurewicz and Watson 1988b) has since enabled workers to use such zonation profiles to determine the thermal history of mantle xenoliths (Takahashi 1980; Köhler and Brey 1990) and the cooling rates of meteorites (Miyamoto et al. 1986). Simpkin and Smith (1970) further suggested that the Ca content in olivine could be pressure dependent. A recent study by Köhler and Brey (1990) calibrated the Ca exchange between olivine and clinopyroxene over a range of pressures and temperatures applicable to the upper mantle and found that this exchange reaction could be successfully used as a geothermobarometer. Experimental studies have also shown that the Ca content of olivine reflects the composition of the silicate liquid with which it equilibrated, and this can be used to assess whether natural olivine was in equilibrium with the host magma (Watson 1979; Jurewicz and Watson 1988a). More recently, Dalton and Wood (1993) found that a relationship existed between the Ca concentration of carbonate melt and the Ca content of olivine and that such a relationship could be useful in identifying mantle xenoliths that have undergone reaction with carbonate melts.

The aim of this study is to characterize the contribution of secondary fluorescence to the detected X-ray signal of Ca during the electron microprobe analysis of olivine near compositional boundaries.

## PREVIOUS STUDIES

Reed and Long (1963) were the first to address both experimentally and theoretically the problem of secondary fluorescence close to grain boundaries. They conducted measurements across an artificial vertical boundary between pure iron and nickel metals at acceleration voltages of 12.5, 15, and 20 kV. At 20 kV they measured 4–5% Fe in Fe-free nickel approximately 4 μm from the boundary, which resulted from secondary fluorescence of Fe X-rays by Ni$K$ X-rays and also from continuum fluorescence. Using a formula modified after Castaing's (1951) fluorescence correction, Reed and Long (1963) then calculated the percent iron in nickel metal at the boundary between the two phases, which should result from secondary fluorescence, both continuum and characteristic. The calculated values were, however, significantly higher than the measured values. No reason for this discrepancy was given, although Adams and Bishop (1986), when using the Reed and Long (1963) formula to calculate the contribution of secondary fluorescence to Ca concentrations in olivine, suggested that spectrometer focus-
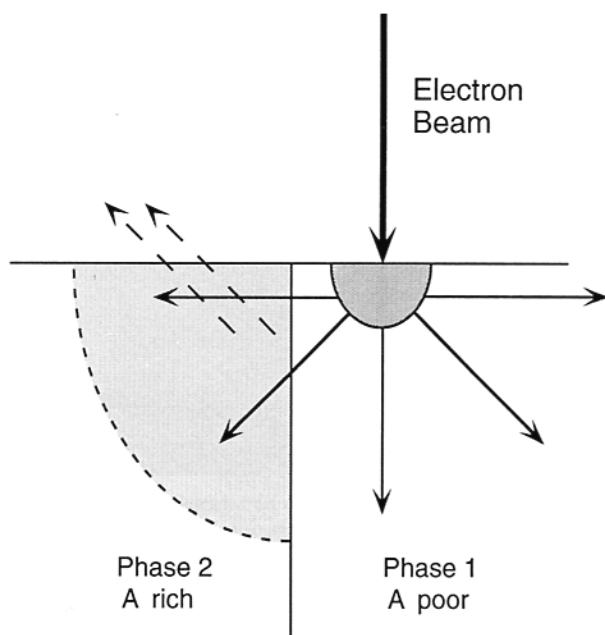


**FIGURE 1.** Electron microprobe analysis of small concentration of $A$ in phase 1 with fluorescence excited in adjoining $A$-rich phase 2. Modified from Reed (1993).

ing could be the cause of the discrepancy. This problem will be addressed in a later section. In an electron microprobe study of Sm partitioning between olivine and synthetic basaltic glasses, McKay (1986, 1989) noted that the Sm concentration in the olivine increased as the interface with the glass (containing approximately 2 wt% Sm) was approached. McKay (1986, 1989) concluded that these apparent concentration gradients were analytical artifacts because they were present even in Sm-free olivine grains that were surrounded by Sm-bearing glass. It was suggested that the excitation of Sm X-rays in the glass, which would increase measured levels of Sm in the olivine, was due to either secondary fluorescence or a significant number of stray electrons from the beam. Regardless of the mechanism, McKay (1986, 1989) recommended that analysis of Sm in the olivine be conducted at least 100 μm from the nearest olivine-glass interface.

A more rigorous attempt to constrain the effects of secondary fluorescence was presented by Bastin et al. (1983, 1984). Following an approach adopted by Henoc et al. (1968), they calculated the effect of characteristic fluorescence of one element by another as a function of distance from the grain boundary. They did this for alloys composed of just two elements joined together with known boundary topography and assumed that there was no contribution from continuum fluorescence to the total fluorescence and that all primary radiation was emitted from a point source located at the specimen surface. Calculations in the system Cu-Co are in reasonable agreement with experiments that they performed on two Cu-Co alloys joined at a straight boundary. The difference

**TABLE 1.** Compositions of minerals used to study secondary fluorescence

| | Olivine (Fo$_{99.5}$)* | Olivine (Fo$_{90.7}$) | Olivine (Fo$_{30}$) | Olivine (Fo$_{8.4}$) | Diopside | Bytownite | Calcite | Glass slide |
|---|---|---|---|---|---|---|---|---|
| Na$_2$O | 0.05(2)** | n.d. | n.d. | n.d. | 0.20(4) | 4.43(13) | — | 12.96(70) |
| MgO | 56.57(45) | 48.81(46) | 12.93(22) | 3.36(13) | 15.89(24) | 0.08(2) | — | 4.00(8) |
| Al$_2$O$_3$ | n.d. | n.d. | n.d. | n.d. | 4.77(11) | 29.06(28) | — | 1.77(8) |
| SiO$_2$ | 42.80(37) | 40.87(34) | 32.57(41) | 29.77(44) | 51.17(40) | 53.30(47) | — | 73.31(68) |
| K$_2$O | n.d. | n.d. | n.d. | n.d. | n.d. | 0.41(4) | — | 0.36(2) |
| CaO | 0.007(7)† | 0.069(7)† | 0.02(1)† | 0.028(5)† | 25.11(19) | 11.92(13) | — | 7.09(14) |
| TiO$_2$ | n.d. | n.d. | n.d. | n.d. | 0.29(4) | 0.07(4) | — | 0.04(3) |
| Cr$_2$O$_3$ | n.d. | n.d. | n.d. | n.d. | n.d. | n.d. | — | n.d. |
| MnO | 0.11(5) | 0.12(6) | n.d. | 1.06(13) | n.d. | n.d. | — | n.d. |
| FeO | 0.49(9) | 8.92(24) | 54.04(58) | 65.56(80) | 2.79(18) | — | — | n.d. |
| Fe$_2$O$_3$ | — | — | — | — | — | 0.36(9) | — | — |
| Fe$_3$O$_4$ | — | — | — | — | — | — | — | — |
| NiO | n.d. | 0.41(6) | n.d. | n.d. | n.d. | n.d. | — | n.d. |
| MgCO$_3$ | — | — | — | — | — | — | 0.25(11) | — |
| CaCO$_3$ | — | — | — | — | — | — | 98.83(96) | — |
| MnCO$_3$ | — | — | — | — | — | — | 0.35(18) | — |
| FeCO$_3$ | — | — | — | — | — | — | 0.27(16) | — |
| Total | 100.12(89) | 99.21(77) | 99.59(72) | 99.81(92) | 100.22(62) | 99.63(68) | 99.70(92) | 99.55(82) |

*Note:* n.d. = not determined.
\* Fo = 100Mg/(Mg + Fe) on a molar basis.
\*\* Numbers in parentheses are two standard deviations of the last digits cited.
† Ca analysis calculated from mean apparent concentrations at distances >150 µm from the interface on couple traverses.

between their calculated and measured values is attributed to continuum fluorescence. No experiments were performed on alloys separated by curved or angular interfaces. On the basis of their calculations Bastin et al. (1983, 1984) suggested a procedure for the correction of secondary fluorescence that can be incorporated into the normal ZAF routine. However, such a correction procedure relies on exact knowledge of the interface geometry between two grains and makes certain assumptions regarding the distance over which the continuum fluorescence is effective. In geological situations the interface geometry is very rarely known, and it must further be remembered that the calculations and modeling of Bastin et al. (1983, 1984) involved just two elements, whereas minerals are dominantly multielement. Taking these points into consideration, the applicability of such models to geologic situations is limited.

Though an accurate knowledge of Ca concentrations in olivine is of clear importance, there has been no systematic study of the range and magnitude of secondary fluorescence of Ca from neighboring phases during electron microprobe analysis. Watson (1979), in a study of the Ca content of forsterite coexisting with silicate liquid, measured Ca concentrations across a boundary between Ca-free synthetic forsterite and Ca-rich silicate glass. The boundaries were fabricated by heating a mechanical mixture of glass and forsterite at 1350 °C for 1 min. This approach generates intimate contact at the interface, but the interface is of unknown topography and the formation of a Ca diffusion profile in the forsterite cannot be ruled out. At a distance of 15 µm from the boundary, Ca X-rays were detectable above background in the forsterite. From this Watson (1979) concluded that measured concentrations of Ca in grains of ≤30 µm would include a contribution from secondary fluorescence. However, the

experiments of Watson (1979) were in an Fe-free system, and so the observed fluorescence in the forsterite was the result of continuum fluorescence only. Jurewicz and Watson (1988a) extended the study of Watson (1979) to Fe-bearing systems. They reported, but did not present, measurements of Ca concentrations across a boundary between natural (Saint Johns Island) olivine and Ca-rich glass. They then used this profile to correct for the effects of secondary fluorescence of Ca in their experimental olivines. However, it is not clear that any precautions were taken to determine the boundary geometry nor to recognize that differences would exist between the interface geometry of the olivine-glass standard and that of the olivine-glass couples in the experiments.

## Experiments

### Approach

The variables likely to control the proportion of detected secondary X-rays were considered to be the following: interface geometry, distance to the interface, Ca content of the neighboring material, and Fe content of the olivine. Variation in analytical conditions, such as accelerating voltage, were not investigated because it is already known that these have little effect (Bastin et al. 1983). To eliminate the effects of variable interface geometry, couples were fabricated with a planar interface perpendicular to the surface. The samples were analyzed for Ca content along a line crossing and perpendicular to the interface. Couples of diopside with either olivine (Fo$_{99.5}$), San Carlos olivine (Fo$_{90.7}$), synthetic olivine (Fo$_{30}$), or olivine (Fo$_{8.4}$) were used to study the effect on secondary fluorescence of Fe content of the olivine. The effect of Ca content of the neighboring material was investigated using couples of San Carlos olivine with either bytownite, diopside, or calcite.

## Sample preparation

The compositions of the minerals used in this study are given in Table 1. The compositions were obtained by averaging a grid of 20 analyses conducted with a 15 nA, 15 kV electron beam with a circular footprint 15 $\mu$m in diameter. Calcite was analyzed according to the methodology presented by Lane and Dalton (1994). Prior to analysis, sample homogeneity was assessed by observation of 25 kV backscattered electron images of each sample and by comparison of the analytical errors expected from X-ray counting statistics with those of the measured data. No image contrast was observed in any of the sample areas analyzed.

To obtain reproducible measurements of the secondary Ca X-ray fluorescence signal, a well-constrained interface geometry is required (Bastin et al. 1983, 1984; Reed 1993). Compositional couples were fabricated with a planar interface perpendicular to the sample surface. Single mineral grains of the relevant phases for each couple were mounted separately in resin. A flat face was lapped onto each mineral grain, which was then diamond polished to 1 $\mu$m. Next, the grains were removed from the resin and the flat faces bonded together with a small drop of resin, producing a planar interface between the two mineral grains. The couple was mounted in a block of resin, which was then sliced perpendicular to the interface, lapped, and finally diamond polished to 1 $\mu$m for analysis. This resulted in two mineral grains separated by a layer of organic resin a few micrometers thick (Fig. 2). The low-density organic layer contained none of the elements of interest and is highly transparent to X-rays capable of fluorescing Ca$K$ X-rays. It should also be noted that the presence of a layer of resin between the two minerals would cause the primary interaction volume to exit the Ca-poor mineral (olivine) before entering the Ca-rich mineral (diopside) when a line of analyses is conducted across the interface, i.e., there is no spatial-averaging effect. This means that the measured concentration of Ca at the interface of the olivine is due entirely to primary excitation of Ca in the olivine, combined with secondary fluorescence from the diopside, and not to primary excitation of Ca in the diopside. This latter phenomenon, better known as the convolution effect, is a result of spatial averaging within the primary interaction volume and has been addressed by Ganguly et al. (1988) with specific application to diffusion profiles in mineral-mineral diffusion couples separated by a vertical interface. However, we shall not consider this effect further because our mineral samples showed no such concentration gradients.

## Method

Measurement of the apparent concentrations of Ca, Mg, Si, and Fe was performed by wavelength-dispersive, electron probe microanalysis using a four-spectrometer JEOL JXA 8600 Superprobe with Link Systems AN 10/85s spectrum analyzer and LEMAS automation at Bristol University. A line of spot analyses, with 2.5 $\mu$m spacing, was made perpendicular to the interface. The standards
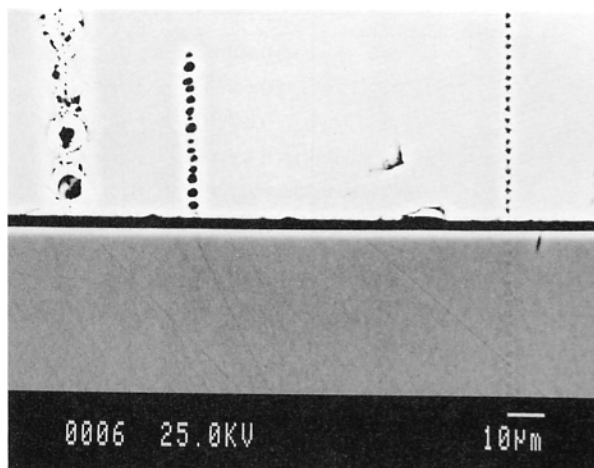


**FIGURE 2.** Backscattered electron micrograph of San Carlos olivine–calcite couple showing the interface between the two phases. Calcite shows physical damage by beams of increasing kilovolts and current. Left traverse = 30 kV, 20 nA; middle traverse = 15 kV, 30 nA; right traverse = 7 kV, 50 nA. All traverses were conducted with a spot beam and 2.5 $\mu$m spacing between each spot. Scale bar is 10 $\mu$m.

were diopside (Ca, Si), Saint Johns Island olivine (Mg), and Fe$_2$O$_3$ (Fe). Sample background and peak count times were 100 s with a beam current of 30 nA and an acceleration voltage of 15 kV. The X-ray data were presented as apparent concentrations without being processed through a correction routine.

McKay (1986, 1989) suggested that stray electrons from the main electron beam may generate significant amounts of X-rays in an adjacent phase up to 100 $\mu$m from the optic axis of the electron microprobe. To test this possibility the edge of a piece of molybdenum foil was stepped across the beam while Mo$L\alpha$ X-rays were counted. When a 30 nA beam struck the foil, X-ray count rates of 5040 $\pm$ 3 s$^{-1}$ were measured at distances >2 $\mu$m from the foil edge. When the beam did not interact directly with the foil but instead passed within >2 $\mu$m of the edge, the X-ray count rate was 0.45 $\pm$ 0.07 s$^{-1}$. The count rate with the electron beam blanked (probe current detector in the beam of the JEOL 8600) was measured at 0.39 $\pm$ 0.06 s$^{-1}$. We conclude from this that no significant flux of electrons strikes the molybdenum foil at distances >2 $\mu$m from the beam center, and that stray electrons do not generate measurable quantities of X-rays for the analytical setup that we used.

X-rays generated by secondary fluorescence of a compositionally different phase than that containing the electron interaction volume can originate several tens of micrometers from the primary interaction volume (Reed and Long 1963). This leads to the possibility of X-rays being generated a significant distance from the Roland circle of the spectrometer. It was discussed earlier that this effect was proposed by Adams and Bishop (1986) to account for the discrepancies between calculated and ex-
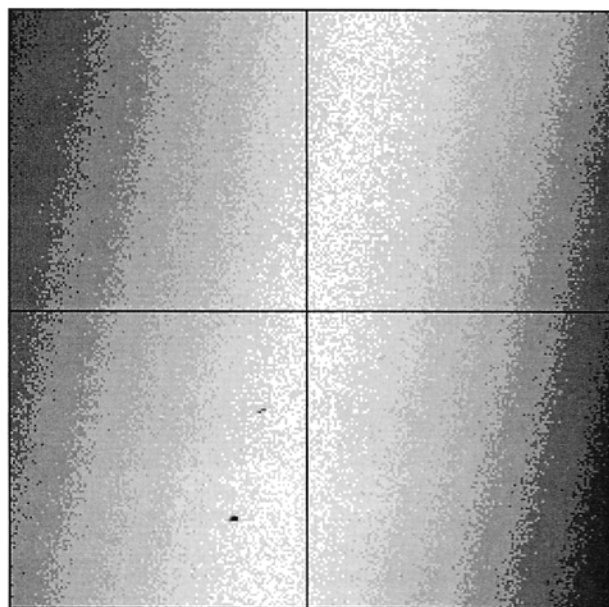
**FIGURE 3.** Scanned beam image of Ca$K\alpha$ X-ray intensity from an andradite crystal using a wavelength-dispersive spectrometer. The image is 400 × 400 $\mu$m, and the cross hairs represent the $x$ (across page) and $y$ (up page) axes of the sample stage, with the cross on the optic axis of the electron optics. Shading represents increasing X-ray counts from black (200 s$^{-1}$) to white (700 s$^{-1}$).

perimentally detected secondary X-rays (Reed and Long 1963). To assess the magnitude of this effect, a digital Ca$K\alpha$ X-ray map was made of an andradite crystal. The Ca X-rays were detected using wavelength-dispersive spectrometer no. 2 equipped with a PET diffracting element and a sealed gas counter with a 330 $\mu$m focusing slit. The image was constructed by stepping the electron beam over a 400 × 400 $\mu$m area to produce a 256 × 256 pixel digital image of detected Ca X-ray intensity. Because the andradite is effectively homogenous in Ca content over the area of the scan, any contrast in the image can be attributed to the geometry of the X-ray source–diffracting element–detector system. Figure 3 shows an eight-level gray scale representation of the image with the $x$ and $y$ stage directions superimposed. This shows a reduction in X-ray counts as the X-ray source is moved away from the focus line of the spectrometer. It can be seen that detection efficiency for X-rays generated in the $x$ direction decreases rapidly with distance, leaving a region of approximately ±30 $\mu$m from the optic axis before significant signal attenuation occurs. Along the $y$ direction, X-rays are detected with almost constant efficiency within 200 $\mu$m of the optic axis. Thus, to minimize the effect of spectrometer defocusing, the samples were oriented within the microprobe with the interface in the $x$ direction. This ensured that secondary fluorescence was sourced in the $y$ direction, where attenuation of the detected signal, because of spectrometer defocusing, was minimized.

## RESULTS

The effect of Fe content of olivine on the secondary fluorescence of Ca from a neighboring diopside grain is shown in Figure 4a. The effects of secondary fluorescence were isolated by subtracting from the measured value the apparent concentration of Ca in each olivine measured at a distance >150 $\mu$m from the interface; the corrected values are presented in Table 1. It is clearly seen in Figure 4a that secondary fluorescence causes enhancement of the apparent concentration of Ca above the $2\sigma$ error (0.005) of the remote concentration of Ca (Table 1) in each olivine as the boundary with diopside is approached. The shapes of the measured curves are in good agreement with those determined for secondary fluorescence in simple binary systems (Reed and Long 1963; Bastin et al. 1983).

The effect of only continuum X-ray fluorescence is effectively demonstrated by the olivine of forsterite content 99.5. A $1\sigma$ increase above the remote measured concentration of Ca occurs within about 60 $\mu$m of the interface. The error exceeds $2\sigma$ at distances <30 $\mu$m from the diopside with a Ca concentration at the interface, due entirely to secondary fluorescence, of 0.04 wt% in comparison with 0.005 wt% at 150 $\mu$m from the interface (Table 1). These data are comparable to those presented by Watson (1979), except that the Ca content of the diopside (18 wt%) is greater than that of the glass (12 wt%) used by Watson (1979). Our data indicate that continuum fluorescence alone creates significant errors in crystals <60 $\mu$m in diameter, twice the value recommended by Watson (1979).

The effect of increasing Fe content, and hence increasing characteristic X-ray fluorescence, is demonstrated by the other three olivine samples in Figure 4a. For all three samples the measured concentration of Ca at the interface is an order of magnitude higher than that at 150 $\mu$m from the interface. For example, the olivine Fo$_{8.4}$ has an apparent concentration of Ca that measures 0.14 wt% at the interface in comparison with 0.02 wt% at a distance of 150 $\mu$m from the interface (Table 1). Figure 4a also shows that noticeable differences in the magnitude of the secondary fluorescence effect between the three olivines of differing Fe content become clear at a distance of <25 $\mu$m from the interface. Regardless of Fe content, however, >$2\sigma$ errors in measured Ca content occur within 45–50 $\mu$m of the interface and warn against analyzing trace amounts of Ca in olivine crystals <100 $\mu$m in diameter.

Figure 4b illustrates the effect of Ca content of the neighboring mineral on secondary fluorescence. The analyzed olivine is the San Carlos olivine (Fo$_{90.7}$, Ca content 0.05 wt%), and the adjoining Ca-rich phase is either bytownite feldspar (8.52 wt% Ca), diopside (17.95 wt% Ca), or calcite (39.58 wt% Ca). We chose the San Carlos olivine because the forsterite content of this olivine resembles that commonly found in nature. As for Figure 4a the effects of secondary fluorescence were isolated by subtracting from the measured value the apparent concen-

tration of Ca in the San Carlos olivine measured at a distance $>150$ $\mu$m from the interface. Also shown in Figure 4b are the results of a traverse across an olivine $(Fo_{90.7})$—olivine $(Fo_{90.7})$ couple, which shows no secondary fluorescence effects because this can be effectively considered a homogeneous sample.

Figure 4b shows that as the Ca concentration of the neighboring mineral increases, the effects of secondary fluorescence become more serious. When the adjoining mineral is bytownite there is a $>2\sigma$ elevation of the Ca signal at distances $<25$ $\mu$m from the interface. This distance increases to 45 $\mu$m for diopside, whereas for calcite the effects of secondary fluorescence cause a $>2\sigma$ increase at distances $<70$ $\mu$m from the interface. The measured Ca concentration of the olivine at the interface with the calcite is $>0.15$ wt% in comparison with 0.05 wt% at a distance of 150 $\mu$m from the interface, a very substantial error. These data indicate that the analysis of trace levels of Ca in an olivine adjacent to a Ca-rich neighbor is reliable only for olivines at least 140 $\mu$m in diameter. In the worst possible case of an Fe-rich olivine adjoining a Ca-rich neighbor we would not recommend analysis for Ca at distances $<100$ $\mu$m from the interface, meaning that the olivine should be at least 200 $\mu$m in diameter.

## DISCUSSION

It has been shown that the combined effects of continuum and characteristic secondary X-ray fluorescence of $CaK$ X-rays lead to substantial errors in the analysis of Ca in olivine close to grain boundaries with Ca-rich phases. The magnitude of the error increases with increasing Fe content of the olivine and Ca content of the neighboring phase (Figs. 4a and 4b). Moreover our experiments were conducted with a known (vertical) interface geometry. If the two grains are separated by a curved boundary or straight boundary inclined toward the olivine then the errors presented in Figures 4a and 4b become more serious. Unfortunately, the case of a curved or inclined interface geometry is that most likely to be encountered in natural and experimentally produced olivines. Rigorous correction procedures for secondary fluorescence, such as those proposed by Bastin et al. (1983, 1984), rely on an exact knowledge of the interface geometry, a quantity that is usually unavailable for geological samples. Adjusting the operating conditions of the electron microprobe does not reduce the effects of secondary fluorescence (Bastin et al. 1984), and we must therefore conclude that without knowledge of boundary geometry the problem is essentially uncorrectable. To obtain reliable concentrations of Ca in olivines that adjoin Ca-rich phases, analyses must be performed in the center of grains at least 50 $\mu$m in diameter for the best-case scenario of an Fe-poor olivine (e.g., $Fo_{90.7}$) adjoining a Ca-poor phase (e.g., bytownite) with a vertical interface between them. For the worst-case scenario of an Fe-rich olivine (e.g., $Fo_{10}$) adjoining a Ca-rich phase such as calcite with a curved boundary separating the two phases, the grain size would have to be at least 200 $\mu$m in di-
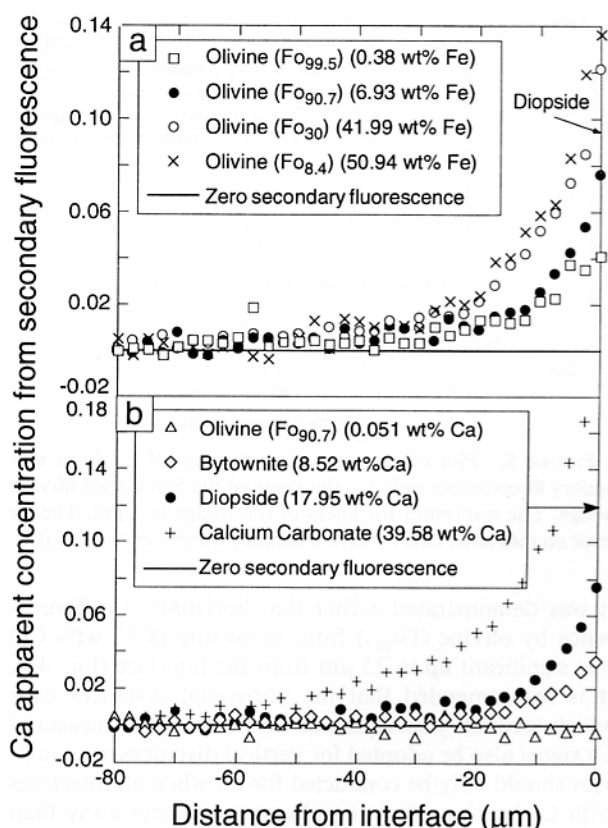


FIGURE 4. Plot of apparent concentration of Ca from secondary fluorescence only vs. distance from interface for (a) couples consisting of diopside and olivine grains of increasing Fe content and (b) couples of San Carlos olivine and minerals of increasing Ca content. The $2\sigma$ error on measured data for zero secondary fluorescence is ±0.005.

ameter. These figures are valid for the X-ray counting statistics used in this study. Analyses of elements at levels of parts per million, in which the number of X-rays counted is much larger, detect the effects of secondary fluorescence at greater distances than those documented here. For example, McKay (1986) detected significant enhancement of parts-per-million concentrations of Sm in olivine at distances of up to 100 $\mu$m from an interface with a glass containing only approximately 2 wt% Sm.

It is common practice to mount most natural geologic samples as 30 $\mu$m thick thin sections on glass slides. An analysis of a typical glass slide is presented in Table 1 and contains 5.06 wt% Ca. To assess the possible effects of secondary fluorescence of Ca from the glass slide as a function of vertical thickness, a wedge of San Carlos olivine mounted on a glass slide was prepared. Minimum wedge thickness was 4 $\mu$m, and the wedge depth increased by 1 $\mu$m every 5 $\mu$m along the horizontal direction. Figure 5 shows the apparent concentration of Ca from secondary fluorescence as a function of wedge thickness. The data show significant ($>2\sigma$ above the remote measured concentration of Ca) Ca secondary fluorescence from the underlying glass slide up to an olivine thickness of 20 $\mu$m.
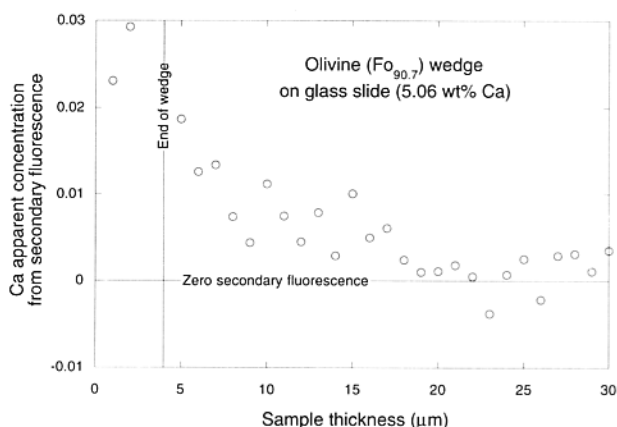
**FIGURE 5.** Plot of apparent concentration of Ca from secondary fluorescence only vs. thickness of the San Carlos olivine wedge. The minimum thickness of the wedge is 4 $\mu$m. The $2\sigma$ error on measured data for zero secondary fluorescence is $\pm0.005$.

It was demonstrated earlier that horizontal Ca fluorescence by olivine (Fo$_{90.7}$) from bytownite (8.52 wt% Ca) was significant up to 25 $\mu$m from the interface (Fig. 4b). It is recommended that the horizontal distances over which secondary fluorescence may add to the measured Ca signal also be adopted for vertical distances, i.e., analyses should only be conducted for Ca when all interfaces with Ca-bearing adjoining phases are farther away than the horizontal radius of the secondary fluorescence interaction volume. To minimize the effect of Ca secondary fluorescence from the slide of a thin section, especially for Fe-rich olivine, it would be prudent to use Ca-free slides.

Olivine commonly displays chemical heterogeneity in Mg, Fe, Ca, and Ni contents, and such heterogeneity is often of interest to geologists. In such cases, an analysis at the center of an olivine grain would not be representative of the olivine as a whole and would provide no information regarding zonation profiles in the olivines. Furthermore, grain sizes in experimental samples rarely attain the sizes recommended above for exclusion of secondary fluorescence effects. We therefore recommend that if one wishes to obtain reliable Ca concentrations and concentration gradients in olivines that adjoin Ca-rich phases, including glass slides, these olivines should be physically separated from the sample, mounted in a Ca-free matrix, and analyzed separately, a practice employed by Köhler and Brey (1990). This procedure is difficult but not impossible for experimental samples. Simply measuring the Ca concentration profile across the interface between an olivine and a Ca-rich phase and using such a profile to correct for secondary X-ray fluorescence of Ca in olivines of varying Fe content next to phases of varying Ca content is insufficient because it assumes that the magnitude of the fluorescence error is the same in all cases, regardless of interface geometry and chemical composition.

**REFERENCES CITED**

Adams, G.E., and Bishop, F.C. (1986) The olivine-clinopyroxene geobarometer: Experimental results in the CaO-FeO-MgO-SiO$_2$ system. Contributions to Mineralogy and Petrology, 94, 230–237.

Bastin, G.F., van Loo, F.J.J., Vosters, P.J.C., and Vrolijk, J.W.G.A. (1983) A correction procedure for characteristic fluorescence encountered in microprobe analysis near phase boundaries. Scanning, 5, 172–183.

———(1984) An iterative procedure for the correction of secondary fluorescence effects in electron-probe microanalysis near phase boundaries. Spectrochimica Acta, 39B(12), 1517–1522.

Castaing, R. (1951) Application des sondes électroniques à une méthode d'analyse ponctuelle chimique et cristallographique. Ph.D. thesis. Paris University, Paris, France.

Dalton, J.A., and Wood, B.J. (1993) The compositions of primary carbonate melts and their evolution through wall-rock reaction in the mantle. Earth and Planetary Science Letters, 119, 511–525.

Ganguly, J., Bhattacharya, R.N., and Chakraborty, S. (1988) Convolution effect in the determination of compositional profiles and diffusion coefficients by microprobe step scans. American Mineralogist, 73, 901–909.

Green, M. (1964) The angular distribution of characteristic X radiation and its origin within a solid target. Proceedings of the Physical Society, 83, 435–451.

Henoc, J., Maurice, F., and Zemskoff, A. (1968) Phénomènes de fluorescence aux limites de phases. In G. Möllenstedt and K.H. Gaukler, Eds., Vth international congress on X-ray optics and microanalysis, p. 187–192, Springer, Berlin.

Jurewicz, A.J.G, and Watson, E.B. (1988a) Cations in olivine: Part I. Calcium partitioning and calcium-magnesium distribution between olivines and coexisting melts, with petrologic applications. Contributions to Mineralogy and Petrology, 99, 176–185.

———(1988b) Cations in olivine: Part 2. Diffusion in olivine xenocrysts, with applications to petrology and mineral physics. Contributions to Mineralogy and Petrology, 99, 186–201.

Köhler, T.P., and Brey, G.P. (1990) Calcium exchange between olivine and clinopyroxene calibrated as a geothermobarometer for natural peridotites from 2 to 60 kb with applications. Geochimica et Cosmochimica Acta, 54, 2375–2388.

Lane, S.J., and Dalton, J.A. (1994) Electron microprobe analysis of geological carbonates. American Mineralogist, 79, 745–749.

McKay, G.A. (1986) Crystal/liquid partitioning of REE in basaltic systems: Extreme fractionation of REE in olivine. Geochimica et Cosmochimica Acta, 50, 69–79.

———(1989) Partitioning of rare earth elements between major silicate minerals and basaltic melts. In Mineralogical Society of America Reviews in Mineralogy, 21, 45–74.

Miyamoto, M., McKay, D.S., McKay, G.A., and Duke, M.B. (1986) Chemical zoning and homogenization of olivines in ordinary chondrites and implication for thermal histories of chondrules. Journal of Geophysical Research, 91(B12), 12804–12816.

Reed, S.J.B. (1993) Electron microprobe analysis (2nd edition), 326 p. Cambridge University Press, Cambridge.

Reed, S.J.B., and Long, J.V.P. (1963) Electron-probe measurements near phase boundaries. In H.H. Patee, V.E. Cosslett, and A. Engström, Eds., 3rd international symposium on X-ray optics and X-ray microanalysis, p. 317–327, Academic, New York.

Simpkin, T., and Smith, J.V. (1970) Minor-element distribution in olivine. Journal of Geology, 78, 304–325.

Stormer, J.C. (1973) Calcium zoning in olivine and its relationship to

silica activity and pressure. Geochimica et Cosmochimica Acta, 37, 1815–1821.

Takahashi, E. (1980) Thermal history of lherzolite xenoliths: I. Petrology of lherzolite xenoliths from the Ichinomegata crater, Oga peninsula, northeast Japan. Geochimica et Cosmochimica Acta, 44, 1643–1658.

Watson, E.B. (1979) Calcium content of forsterite coexisting with silicate liquid in the system $Na_2O$-CaO-MgO-$Al_2O_3$-$SiO_2$. American Mineralogist, 64, 824–829.